ELSEVIER

Journal of Non-Crystalline Solids 279 (2001) 44–50

JOURNAL OF NON-CRYSTALLINE SOLIDS

www.elsevier.com/locate/jnoncrysol

Crack growth behavior of zinc tellurite glass with or without sodium oxide

Satoshi Yoshida *, Jun Matsuoka, Naohiro Soga

Department of Materials Science, School of Engineering, The University of Shiga Prefecture, 2500 Hassaka, Hikone, Shiga 522-8533, Japan

Received 5 April 2000

Abstract

The crack growth behavior was investigated for zinc tellurite glasses with or without sodium oxide by using a small-size double cleavage drilled compression (DCDC) specimen, which was a rectangular bar with a small hole in the middle. The sample dimensions used were about a half or less than those of the previous studies, and comparable with those of JIS specimen for flexural strength testing. The validity of applying such a small specimen for test was examined on a commercial soda-lime silicate glass, and it was found feasible to obtain the data and to discuss crack growth behavior of glass. By using this small-size DCDC specimen, $K_I - v$ curves for tellurite glasses were successfully obtained for the first time. It was found that $K_I - v$ curves showed three characteristic regions similar to silicate glasses, but they shifted considerably toward the low K_I side, reflecting much weaker bond-strength of tellurite glass than silicate glass. The fatigue parameter for tellurite glass was much larger than that for commercial silicate glass. This large fatigue parameter of tellurite glass was considered to result from a relatively small contribution of stress corrosion reaction to the subcritical crack growth because of the narrow distribution of bond-strength caused by the lack of ring structures in tellurite glass.

1. Introduction

Stress corrosion and delayed failure in glass are very important for evaluating the reliability and long-term durability of glass. For glass and glass-related materials, it is well known that subcritical crack growth occurs in corrosive environments such as water, ammonia, moist air below the critical fracture stress. This subcritical crack growth is the main reason for delayed failure in glass in such environment. The pioneering work on subcritical crack growth in glass was carried out by Wiederhorn [1] in moist N_2 environment, and clarified the existence of three characteristic regions in the crack velocity curve under the subcritical fracture stress, when the log crack velocity, v, is plotted against the log stress intensity factor, K_I, as shown in Fig. 1. Among these three characteristic regions, the crack growth in region I is considered to be controlled by the reaction rate between Si–O–Si bond and corrosive species, such as water, and that in region II by the rate of transport of corrosive species to the crack tip. On the other hand, the crack growth in region III is independent of the presence of corrosive species, which suggests that the crack motion in this region is related to the intrinsic crack growth in glass. Since the crack

* Corresponding author. Tel.: +81-749 28 8366; fax: +81-749 28 8596.

E-mail address: yoshida@mat.usp.ac.jp (S. Yoshida).

0022-3093/01/$ - see front matter
PII: S0022-3093(00)00395-1

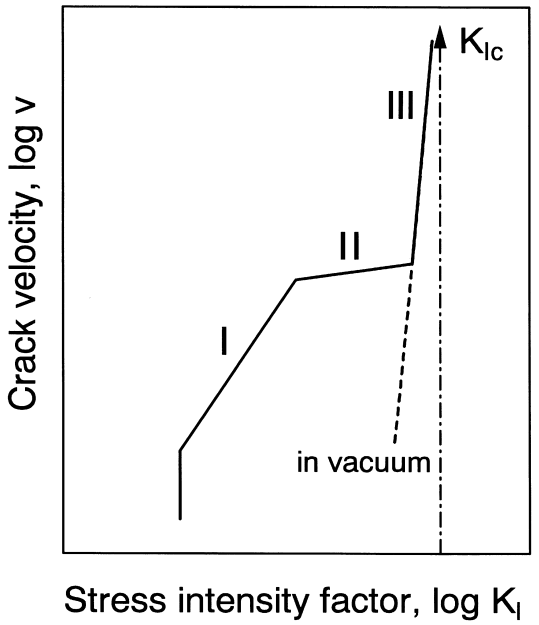

Fig. 1. Schematic diagram of stress intensity factor, K_I, and crack velocity, v. K_{Ic} is the critical stress intensity factor, that is fracture toughness. Dashed line denotes $K_I - v$ curve in vacuum or in inert environment.

growth curve in glass gives meaningful information about delayed failure caused by the stress-assisted chemical reaction, a number of investigations [2–5] followed this work in different environmental conditions and some microscopic mechanisms of stress corrosion reaction have been proposed [6]. However, most of the glasses investigated previously are limited to commercial silicate glasses, mostly because of difficulty in preparing glass specimens for crack growth experiments. Consequently, there exists no report on new types of glasses, such as tellurite glasses, which have been counted upon for new optical devices, such as an optical fiber amplifier [7]. One way to overcome such a difficulty is to utilize a small-size specimen. In the previous study [8], we followed Janssen's work [9] and applied double cleavage drilled compression (DCDC) specimens to measure relatively high crack velocities in region III and confirmed the advantage of simple sample geometry and crack stability over the double cantilever beam (DCB) or double torsion (DT) methods. Other investigators have also used DCDC specimens to study the subcritical crack growth behavior in commercial phosphate laser glass by using DCDC specimens [10,11]. They mentioned that other types of fracture specimens could not be used for a phosphate laser glass because of their lower fracture toughness.

The purpose of the present study is twofold: (1) to evaluate the applicability of a smaller DCDC specimen than those reported previously, and (2) to evaluate the crack growth behavior of tellurite glass. The small-size DCDC specimen employed was square cross-sectioned rod with a circular hole drilled in its center as shown in Fig. 2, having the dimensions of $L = 35$ mm, $w = 3.5$ mm, $d = 3$ mm, and the hole radius, $R = 0.5$ mm (nominal). These dimensions were almost comparable with those of JIS specimens for flexural strength testing [12] and fracture toughness testing of high performance ceramics [13], which were $L = 36$ mm, $w = 4$ mm, $d = 3$ mm, and about a half size of our previous samples [8] ($L = 70$ mm, $w = 7$ mm, $d = 6$ mm, and the hole radius, $R = 1$ mm (nominal)) or those of Michalske et al. [14–16] and other investigators [9,10] ($L = 75$ mm, $w = 7.5$ mm, $d = 6.5$ mm, and

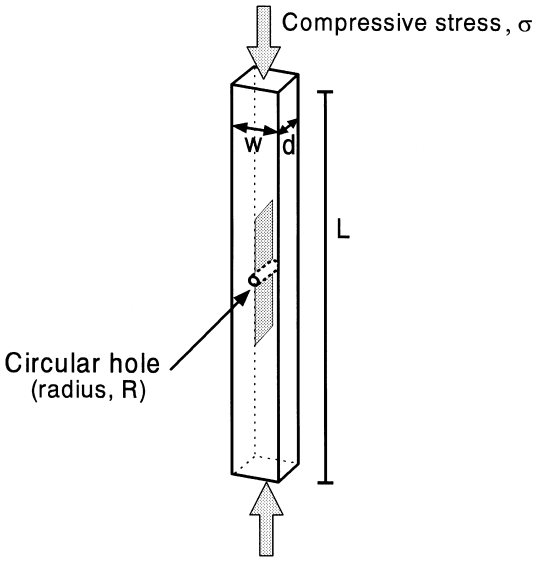

Fig. 2. The DCDC specimen geometry. The dimensions were $L = 35$ mm, $w = 3.5$ mm, $d = 3$ mm, and the radius of hole, $R = 0.5$ mm (nominal). Two cracks propagate from the center hole along the long axis of the specimen under compressive stress.

Table 1
Various dimensions and volumes of the specimens for evaluating $K_I - v$ diagram

Specimen		Dimension (mm)	Volume (mm^3)
DCB	Wiederhorn and Bolz [17]	$75 \times 25 \times 2$	3750
DCB	Freiman [18]	$51 \times 13 \times 1$	663
DT	Soga et al. [19]	$70 \times 16 \times 1.6$	1792
CT (compact tension)	Sakaguchi et al. [5]	$48 \times 50 \times 2.5$	6000
CN (Chevron notched)	Shiono et al. [20]	$100 \times 5 \times 5$	2500
DCDC	Janssen [9]	$150 \times 15 \times 15$	33 750
DCDC	Michalske and Fuller [14]	$75 \times 7.5 \times 6.5$	3656
Glass fiber[a]	Muraoka and Abé [21]	$\phi 0.125 \times 50$	0.614
DCDC	This study	$35 \times 3.5 \times 3$	368

[a] Crack velocity, $v < 10^{-5}$ m/s.

the hole radius, $R = 1$ mm (nominal)). The dimensions of Janssen's original DCDC specimen were $L = 150$ mm, $w = 15$ mm, $d = 15$ mm, and $R = 2$ mm [9]. In Table 1, the dimensions and volumes of the specimens used previously for evaluating $K_I - v$ curve are summarized. To test the feasibility of small-size DCDC specimens, the $K_I - v$ curves of soda-lime silicate glass were determined on two different size specimens and compared with those obtained by different methods.

2. Experimental procedures

The glasses employed in this study were three types: a commercial soda-lime silicate glass, zinc tellurite glass ($30ZnO–70TeO_2$), and sodium zinc tellurite glass ($20Na_2O–10ZnO–70TeO_2$). Tellurite glasses were prepared from reagent-grade Na_2CO_3, ZnO, and TeO_2. The powders weighed appropriately were mixed thoroughly and melted in Pt–Au crucibles at 800°C for 20 min in an electric furnace. The resultant glasses were annealed at $T_g + 10$°C depending on the composition for 30 min and cooled to room temperature in the furnace and then shaped to the required size. The samples were loaded in compression with a closed-loop mechanical testing machine (Instron 1362). The compression load was increased at a compression rate of 0.05 mm/s until auto pre-cracking was achieved. In some cases of tellurite glasses, an appropriate load was kept until pre-crack was formed, because a short-length pre-crack was not achieved in this process. A series of compressive load pulses with various duration times and with various maximum load values were applied to propagate the crack. A small load (250 N for soda-lime silicate glass, 160 N for sodium zinc tellurite glasses), by which the crack could not extend, was superposed on the specimen during the experiment as a bias load. The crack in the specimen was able to propagate only during each load pulse. These experiments were carried out in air, 25°C ± 2°C, 60%RH ±10%.

The crack front was measured by the displacement analyzer with a video monitor. The position of the crack front was detected with the aid of polarized light for soda-lime silicate glass and ordinary light for tellurite glasses. The cursor of displacement analyzer gave the transverse position in the video frame divided into 640 channels. As the actual transverse length in the video frame was about 7 mm, which corresponded to a magnification of 40×, it was possible to determine the position of the crack front with an accuracy of only 0.01 mm. The video recorder was able to restore frames every 1/30 s, so higher crack velocities $>10^{-4}$ m/s could be measured.

In the present study, the stress intensity factor (K_I) at a given velocity was calculated from the applied stress and crack length using the following equation based on finite element calculation by He et al. [22],

$$\frac{\sigma(\pi R)^{1/2}}{K_I} = \frac{w}{2R} + \left(0.235\frac{w}{2R} - 0.259\right)\frac{a}{R}, \qquad (1)$$

where σ is the applied compressive stress, R the radius of hole, K_I the stress intensity factor at

mode I, w the specimen width, and a is the crack length. Michalske et al. [15] reported the almost same relationship between the stress intensity factor and the crack length for DCDC specimen by the same finite element calculation code, but their results were obtained for only two geometries, $w/R = 7.5$ and $w/R = 6.25$. In addition, the calculated results obtained by He et al., (Eq. (1)) were much closer to the experimental calibration data by Michalske et al. For the sample geometry of $w/R = 7.5$, the agreement between the calculated and the experimental calibration values were within 5% for the results by He et al., and within 9% for the results by Michalske et al., respectively.

3. Results

Fig. 3 shows $K_I - v$ diagram for commercial soda-lime silicate glass. Closed circles are data obtained in air at 25°C and 60%RH by using small DCDC specimens (this study). Open circles are data from large specimens reported previously [8].

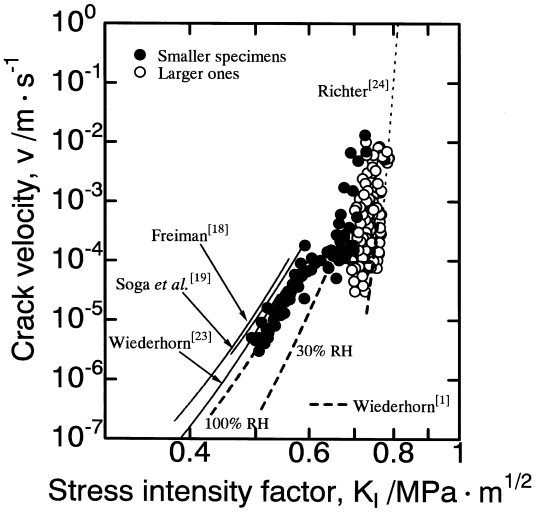

Fig. 3. $K_I - v$ diagram for commercial soda-lime silicate glass. Closed circles are data obtained in air at 25°C and 60% by using smaller DCDC specimens (this study). Open circles are data from larger specimens reported previously [8]. The dashed lines represent the crack growth curve obtained in moist nitrogen by Wiederhorn [1]. The dotted line represents region III in $K_I - v$ curve by Richter [24]. The solid lines denote previous results in water (after [18,19,23]).

All of the data points obtained from three separate specimens are plotted in the figure. The dashed lines denote replotted $K_I - v$ curves reported by Wiederhorn [1], which were obtained by using conventional DCB specimens in moist N_2 environment. The solid lines denote some reported $K_I - v$ curves by others for soda-lime silicate glasses in water. The fine dotted line denotes the $K_I - v$ curve obtained by using stress wave fractography technique with a single edge notched specimen in air, where relative humidity in their experiment was not known [24]. As shown in Fig. 3, $K_I - v$ data obtained here by using DCDC specimens are reasonably consistent with those reported with respect to their slope and their position, and show the characteristic three regions described above. However, the high crack velocity data obtained for the smaller specimen in this study seem to deviate by 6–8% from those for the larger one.

Fig. 4 shows the $K_I - v$ diagram for sodium zinc tellurite glasses. Data points are obtained from at least two specimens for each composition. In order to discuss the crack growth behavior of glass, the data are usually fit to the empirical equation

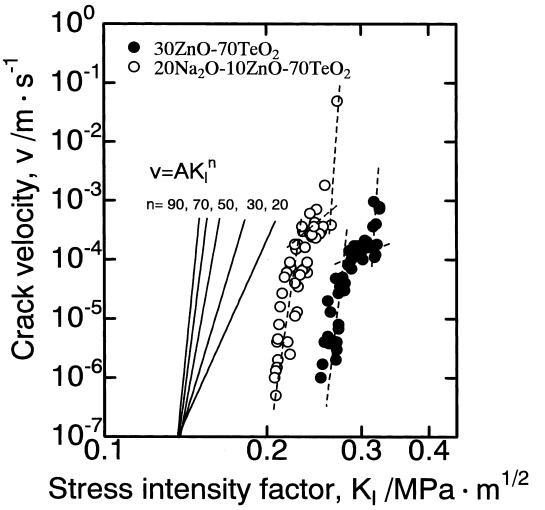

Fig. 4. $K_I - v$ diagram for sodium zinc tellurite glasses. All the data were obtained in air at 25°C and 60%. The solid lines denote some hypothetical $K_I - v$ slopes. Dashed lines are drawn as guides for the eye.

$$v = AK_I^n, \quad (2)$$

where A and n are constants, and n is called as the fatigue parameter. In Fig. 4, some hypothetical $K_I - v$ slopes are indicated as solid lines. Dashed lines are drawn as guides for the eye. The $K_I - v$ curves for tellurite glasses show three characteristic regions similar to those of silicate glass. For both tellurite glasses, the plateau region corresponding to region II in Fig. 1 appears around 10^{-4} m/s. This suggests that the crack growth in tellurite glass is influenced by a chemical reaction between glass network and water vapor in the environment, in a similar manner as silicate glasses and phosphate laser glass [10,11].

4. Discussion

4.1. Evaluation of crack growth for a small-size DCDC specimen

In Fig. 3, the high crack velocity data obtained for the smaller specimen in this study deviated 6–8% from those for the larger one. Although this discrepancy may be critical to discuss the energy barrier for breaking the chemical bonds, the data obtained on a small-size DCDC specimen is considered suitable to discuss the crack growth behavior in glass because of its low scatter and repeatability of data points. The origin of this discrepancy is not clear at this moment. It may arise from the differential in the size of the specimen or the ratio of the specimen width to the center hole radius. As for the ratio of the specimen width to the center hole radius, w/R, the smaller specimen had a slightly different value from the larger one because of the limitation of drill size and processing accuracy, 1.2 mm for the smaller specimen and 2.2 mm for the larger one. The values of w/R for the smaller specimen and for the larger one were approximately 5.8 and 6.4, respectively. Michalske et al. [15] reported that the larger value of w/R made K_I larger, up to 9% from the experimental calibration values. In their case, the calculated stress intensity factors were about 8% larger than the experimental calibration values for the geometry, $w/R = 7.5$. On the other hand, for the other geometry ($w/R = 6.25$), the calculated stress intensity factors were about 4% larger than the experimental calibration values. This size effect would be one origin of the discrepancy between $K_I - v$ data for the smaller specimen and those for the larger one. Further detailed experiments with the specimens having various ratios of w/R and another finite element analysis considering the specimen geometry are necessary to clarify the size effect on stress intensity calibration.

4.2. Crack growth behavior in sodium zinc tellurite glasses

In Figs. 3 and 4, the comparison in $K_I - v$ curves, particularly regions I and III, between silicate glass and tellurite glass shows some distinct differences arising from the difference in bond-strength. Firstly, $K_I - v$ curves for tellurite glasses are located in much lower stress intensity factor than that for silicate glass, indicating that tellurite glasses are more brittle than silicates. The degree of the shift of region III is comparable to the change in the fracture toughness. Watanabe et al. [25] reported K_c value of TeO_2-based glass ($10K_2O$–$20WO_3$–$70TeO_2$) as 0.23 MPa $m^{1/2}$ by using an indentation technique, which was much lower than that of commercial soda-lime silicate glass [26], 0.75 MPa $m^{1/2}$. Secondly, the substitution of ZnO by Na_2O in tellurite glasses caused $K_I - v$ curve to be shifted toward lower stress intensity, and region II to be shorter and ambiguous. This variation of $K_I - v$ curve with Na_2O content may be interpreted by a decrease in bond-strength with introduction of weak non-bridging Na–O bonds. Weakening of averaging bond-strength or weak points in glass structure shifts the $K_I - v$ curve toward the low stress intensity side, especially in region III where the crack growth is caused by the intrinsic bond rupture. The diminishment of region II in $K_I - v$ curve for tellurite glass with addition of Na_2O is caused by the smaller effect of glass composition on the position of region I in $K_I - v$ curve than on that of region III. Thirdly, the slopes of $K_I - v$ curve in region I for tellurite glasses ($n = 50$–70), which are fatigue parameters, are much larger than those for silicate glasses ($n = 10$–30) [27]. This shows a relatively small contribution of stress corrosion

reaction to the subcritical crack growth in tellurite glass. The stress corrosion mechanism is based upon a stress enhanced chemical reaction between water and chemical bond in glass [6]. A strained bond is less stable and thus more susceptible to stress corrosion. For silica and silicate glasses, the strained ring structures have been reported to affect much of the chemical reaction between Si–O–Si bond and water [28]. West and Hench [28] concluded that the nature of the subcritical crack growth in region I was controlled by hydrolysis of three membered rings in silica glass where the energy barrier for pentacoordinate hydrolysis was only 7 kcal/mol. It has also been reported that higher strain energy of three membered ring in silica glass was originated from the smaller angles of Si–O–Si bond and O–Si–O bond [29]. These strained bonds are considered to cause the bond rupture by hydrolysis under much lower stress than the fracture stress. In tellurite glass, on the other hand, such ring structures have not been found. Bürger et al. [30] suggest the existence of a chain-like structure in $20ZnO–80TeO_2$ glass in accord with the chain-like structure of crystalline $Zn_2Te_3O_8$ from the result of neutron diffraction. Probably, such a chain-like structure cannot permit the strained bonds. As a result, the distribution of bond-strength in the chain structure of tellurite glass is narrower than those of silica and silicate glass, causing higher fatigue parameter in tellurite glass. Such high fatigue parameters have been also reported for fluoride glass (ZBLAN, $n \sim 75$) [27] and for phosphate laser glass ($n = 30$–50 estimated from the data points) [11].

5. Conclusion

The crack growth behavior of tellurite glass was successfully evaluated with a small-size DCDC specimen with almost comparable size of JIS specimens for flexural strength testing and fracture toughness testing. Such a small-size specimen is valuable for evaluating $K_I - v$ curve for laboratory-made glass. The $K_I - v$ curves for zinc tellurite glasses with or without sodium oxide showed three characteristic regions just as those for silicate glass. However, $K_I - v$ curves for tellurite glasses were located in much lower stress intensity factor than those for silicate glasses. The slope of $K_I - v$ curve for tellurite glasses ($n = 50$–70) was much larger than those for silicate glasses ($n = 10$–30), which is considered to have originated from relatively small contribution of stress corrosion reaction to the subcritical crack growth because of the narrow distribution of bond-strength in tellurite glass, resulting from the lack of the ring structures.

Acknowledgements

This work is supported by a Grant-in-Aid for Scientific Research from Ministry of Education, Science, Culture and Sport, Japan.

References

[1] S.M. Wiederhorn, J. Am. Ceram. Soc. 50 (1967) 407.
[2] A.G. Evans, J. Mater. Sci. 7 (1972) 1137.
[3] S.W. Freiman, D.R. Mulville, P.W. Mast, J. Mater. Sci. 8 (1973) 1527.
[4] C.J. Simmons, S.W. Freiman, J. Am. Ceram. Soc. 64 (1981) 684.
[5] S. Sakaguchi, Y. Sawaki, Y. Abe, T. Kawasaki, J. Mater. Sci. 17 (1982) 2878.
[6] T.A. Michalske, S.W. Freiman, J. Am. Ceram. Soc. 66 (1983) 284.
[7] J.S. Wang, E.M. Vogel, E. Snitzer, Opt. Mater. 3 (1994) 187.
[8] S. Yoshida, J. Matsuoka, N. Soga, J. Am. Ceram. Soc. 82 (1999) 1621.
[9] C. Janssen, in: Proceedings of the 10th International Congress on Glass, vol. 10, Kyoto, Japan, 1974, p. 23.
[10] Y.-K. Lee, M. Tomozawa, J. Non-Cryst. Solids 248 (1999) 203.
[11] S.N. Crichton, M. Tomozawa, J. Am. Ceram. Soc. 82 (1999) 3097.
[12] Japanese Industrial Standards, Reports 1601, 1981.
[13] Japanese Industrial Standards, Reports 1607, 1990.
[14] T.A. Michalske, E.R. Fuller Jr., J. Am. Ceram. Soc. 68 (1985) 586.
[15] T.A. Michalske, W.L. Smith, E.P. Chen, Eng. Frac. Mech. 45 (1993) 637.
[16] T.A. Michalske, W.L. Smith, J.E. Houston, J. Appl. Phys. 76 (1994) 2109.
[17] S.M. Wiederhorn, L.H. Bolz, J. Am. Ceram. Soc. 53 (1970) 543.
[18] S.W. Freiman, J. Am. Ceram. Soc. 57 (1974) 350.
[19] N. Soga, T. Okamoto, T. Hanada, M. Kunugi, J. Am. Ceram. Soc. 62 (1979) 309.

[20] T. Shiono, R. Ota, N. Soga, J. Soc. Mater. Sci. Japan 32 (1983) 1254 (in Japanese).
[21] M. Muraoka, H. Abé, J. Am. Ceram. Soc. 79 (1996) 51.
[22] M.Y. He, M.R. Turner, A.G. Evans, Acta Metall. Mater. 43 (1995) 3453.
[23] S.M. Wiederhorn, H. Johnson, J. Am. Ceram. Soc. 56 (1973) 192.
[24] H. Richter, in: C.R. Kurkjian (Ed.), Strength of Inorganic Glass, Plenum, New York, 1985, p. 219.
[25] T. Watanabe, Y. Benino, K. Ishizaki, T. Komatsu, J. Ceram. Soc. Japan 107 (1999) 1140.
[26] J. Sehgal, S. Ito, J. Am. Ceram. Soc. 81 (1998) 2485.
[27] S.W. Freiman, in: R.H. Jones (Ed.), Stress-Corrosion Cracking, ASM International, Metals Park, OH, 1992, p. 337.
[28] J.K. West, L.L. Hench, J. Mater. Sci. 29 (1994) 5808.
[29] J.P. Rino, I. Ebbsjö, R.K. Kalia, A. Nakano, P. Vashishta, Phys. Rev. B 47 (1993) 3053.
[30] H. Bürger, K. Kneipp, H. Hobert, W. Vogel, V. Kozhukharov, S. Neov, J. Non-Cryst. Solids 151 (1992) 134.